applied sciences

MDPI

Article

Aerothermoelastic Analysis of Conical Shell in Supersonic Flow

Min Wang [1], Leilei Zeng [1], Changying Zhao [2], Shupeng Sun [2,*] and Yang Yang [3]

[1] AVIC Research Institute for Special Structures of Aeronautical Composites, Jinan 250104, China
[2] Department of Engineering Mechanics, Shandong University, Jinan 250061, China
[3] School of Mechanics and Aerospace Engineering, Southwest Jiaotong University, Chengdu 610031, China
* Correspondence: shpsun@sdu.edu.cn; Tel.: +86-(0)531-88392812

Abstract: The aerothermoelastic behavior of a conical shell in supersonic flow is studied in the paper. According to Love's first approximation shell theory, the kinetic energy and strain energy of the conical shell are expressed and the aerodynamic model is established by using the linear piston theory with a curvature correction term. By taking the characteristic orthogonal polynomial series as the admissible functions, the mode function of conical shell under different boundary conditions can be obtained using the Rayleigh–Ritz method. Then, the dynamic model of the conical shell is derived by using the Lagrange equation. Based on the model, variations in the natural frequencies with respect to temperature and free-stream static pressure are analyzed. Additionally, the effects of the length-to-radius ratio, the thickness-to-radius ratio, and semi-vertex angle, as well as the thermal and aerodynamic loads on the aerothermoelastic stability of the structure are investigated in detail.

Keywords: aerothermoelasticity; flutter; conical shell; general constraint

Citation: Wang, M.; Zeng, L.; Zhao, C.; Sun, S.; Yang, Y. Aerothermoelastic Analysis of Conical Shell in Supersonic Flow. *Appl. Sci.* **2023**, *13*, 4850. https://doi.org/10.3390/app13084850

Academic Editor: Angelo Luongo

Received: 25 February 2023
Revised: 30 March 2023
Accepted: 10 April 2023
Published: 12 April 2023

1. Introduction

Due to its beneficial aerodynamic shape and mechanical properties, the conical shell is widely used in the structural component of supersonic vehicles, such as the nose cones of supersonic missiles and aircraft radomes. During high-speed flight, these components, which are subjected to aerodynamic loads and aerodynamic heating, may experience aerothermoelastic instability, which can damage the structure. Therefore, it is necessary to investigate the aerothermoelastic behavior of the conical shell in supersonic flow.

Many scholars have studied the vibration characteristics of shell of revolution, considering aerodynamic load and aerodynamic heating. Among them, the supersonic flutter and aerothermoelastic behavior of cylindrical shells has been studied extensively and carefully. Based on Donnell's nonlinear shell theory and Galerkin's solution procedure, Amabili and Pellicano [1,2] analyzed both the linear and nonlinear aeroelastic stability of circular cylindrical shells under supersonic airflow. Haddadpour [3] analyzed the supersonic flutter of a composite cylindrical shell under simply supported boundaries at both ends. The influence of temperature change on aeroelastic stability was explored with varied values of the power-law index. The aerothermoelastic characteristics of a composite cylindrical shell were studied by Shin et al. [4], wherein the theory of the layer-wise displacement field was used for various damping treatments, and the post-buckling behaviors and aeroelastic characteristics were investigated with various damping treatments. Based on the frequency–domain and time–domain methods, Song and Li [5] conducted a study of the aerothermoelastic characteristics of a cylindrical shell made from laminated composite material. The effect of the direction of fiber laying on the flutter performance and buckling under heating conditions was studied. By combining the Sanders shell theory with a classical finite element method, Sabri and Lakis [6] proposed a hybrid finite element method to investigate the aerothermoelasticity of a functionally graded cylindrical shell, and analyzed the effects of internal pressure and temperature change on the aeroelastic stability. According to the virtual displacement principle, Bochkarev et al. [7] explored the aeroelastic

behavior of a heated cylindrical shell made from composite material under the combined action of internal and external air flows with clamped–clamped boundaries. The effects of material properties, aerodynamic loads and thermal loads on the flutter boundary were analyzed. Asadi [8] explored for the first time the aerothermoelastic stability of a cylindrical shell made from functionally graded carbon nanotube-reinforced composite material. The influence of various influential factors on the aerothermoelastic stability was investigated in detail. Additionally, taking a functionally graded carbon nanotube-reinforced composite cylindrical shell as the research object, Zhang et al. [9] analyzed the aerothermoelastic behavior of a cylindrical shell based on the frequency–domain method. In addition, the effect of varied control methods on active flutter control was also studied. Chai et al. [10] adopted Hamilton's principle to establish a dynamic model of a composite laminated cylindrical shell. Based on the equation of motion, the aerothermoelastic behavior of the cylindrical shell with the elastic boundaries was studied. The effects of different directions of spring constant on thermal buckling and aeroelasticity stability were investigated in detail. Lin et al. [11] explored the vibration behavior and flutter stability of a composite cylindrical shell under varied boundary conditions by using the same method as mentioned above. Bochkarev [12] decided to study the aerothermoelastic characteristics of a loaded functionally graded circular cylindrical shell under the action of supersonic airflow. The influence of the different combination of mechanical, thermal and aerodynamic loads on the stability of the structure was analyzed. By using the improved differential quadrature method, which is a numerical approximation method, Fazilati et al. [13] explored the aerothermo-elastic characteristics of functionally graded cylindrical curved panels under high supersonic airflow. The impact of temperature change, Mach number and other environmental factors on structure flutter response was emphasized. Mahmoudkhani [14] used the Newton–Raphson method to study the aerothermoelastic stability of a composite cylindrical shell in a thermal environment. The effects of axisymmetric and asymmetric geometrical defects on aerothermoelastic stability were considered. Based on the first-order piston theory and the quasi-steady-state thermal stress theory, Guo et al. [15] explored the post-buckling and flutter behavior of composite cylindrical panels in supersonic airflow in a thermal field, based on the least-square Ritz method. According to the literature review above, piston theory is an effective theory for calculating aerodynamic models in supersonic airflow. The scope and limitation of its application are studied in [16–19].

For conical shells, numerous articles reported the vibration characteristics considering thermal load [20–23] and aerodynamic load [24–32], individually. Bhangale et al. [20] explored the thermal buckling of conical shells composed of advanced composite material by using a semi-analytic finite element method under the clamped–clamped boundary conditions. The influence of material performance and geometric parameters on thermal buckling behavior was studied. Naj et al. [21] mainly investigated the thermal buckling characteristics of composite conical shells with simply supported boundaries at both ends. Talebitooti [22] explored the effect of thermal load on the vibration behavior of a ring-stiffened rotating conical shell composed of functionally graded material under a clamped–clamped boundary conditions. Based on the generalized differential quadrature method, Shakouri [23] studied the vibration behavior of rotating conical shells in a thermal environment. Utilizing Donnell's shell theory, Dixon and Hudson [24] investigated the flutter, vibration and buckling of a conical shell using the generalized Galerkin method. In the modeling process, the in-plane inertias and structural damping were neglected, and the aerodynamic loading was established by inviscid two-dimensional quasi-steady approximation. Bismarcknasr and Costasavio [25] first used the finite-element method to analyze the supersonic flutter of conical shells. According to a new formulation for calculating aerodynamic loads, considering quasi-static pressure and including the terms of added mass, rotational inertia and the forces in the midplane, Vasil'ev [26] analyzed the flutter problem of the conical shell and discussed the effect degree of the terms on the critical Mach number. Sabri and Lakis [27] established an aeroelastic model of a conical shell according to the hybrid finite element method, and analyzed the flutter stability

of the structure with different boundary conditions and a semi-vertex angle. With the differential quadrature method, the effects of the geometric parameters of conical shells, aerodynamic damping and the piston curvature correction term on the flutter stability of a conical shell were investigated by Zhang et al. [28]. Mehri et al. [29] mainly investigated the aeroelasticity of conical shells under yaw supersonic flow. The effects of material properties, geometric parameters, and aerodynamic loads on flutter boundaries have been explored in detail. Bakhtiari et al. [30] investigated the linear and nonlinear flutter stability of truncated conical shells under the influence of supersonic airflow. With Hamilton's principle, the effects of the mass fraction, agglomeration parameters and distribution pattern of the agglomerated carbon nanotubes on aeroelastic stability were investigated by Afshari et al. [31]. Rahmanian and Javadi [32] studied the aeroelasticity of a conical shell under yaw supersonic flow.

However, there is little literature on aerothermoelastic analysis of conical shells. Mahmoudkhani et al. [33] investigated the aerothermoelastic stability of a composite truncated conical shell under simply supported boundary conditions in supersonic airflow. According to the displacements given by double trigonometric series, Hao et al. [34] analyzed the nonlinear vibration of a conical shell which was subjected to aerodynamic load and thermal load under simply supported boundaries. During the modeling process, the displacement components were approximate, and the governing equations of motion ignored the effect of in-plane inertia. For conical shells with simply supported boundary conditions, the double trigonometric function can be used as the trial function, and the results obtained are acceptable. However, obtaining simple trial functions for more general constraints is challenging, which limits further study of the vibration characteristics of conical shells.

It can be noted from the above review that at present, the aerothermoelastic analysis of conical shells is mainly focused on conical shells with simply supported boundaries, and there is a lack of aerothermoelastic research on conical shells with more general constraints. Therefore, in the present paper, the aerothermoelastic characteristics of a functionally graded conical shell with classical boundary conditions in supersonic flow are investigated. Based on Love's shell theory, the kinetic energy and potential energy of the conical shell are obtained. According to the linearized first-order potential theory and the temperature assumption along the thickness direction, the aerodynamic loads and thermal loads are calculated. By taking the characteristic orthogonal polynomial series which are constructed using a Gram–Schmidt procedure as the admissible functions, the mode function of the conical shell is obtained using the Rayleigh–Ritz method. The dynamical equation of the functionally graded conical shell is established by a Lagrange equation. Taking conical shells under free–clamped boundaries as the research object, the effects of thermal and aerodynamic loads on natural vibration characteristics are analyzed. Then, on this basis, the effects of length-to-radius ratio, thickness-to-radius ratio, semi-vertex angle, aerodynamic load and thermal load on the aerothermoelastic stability of conical shells are investigated.

2. Dynamic Model

2.1. Model Description

As shown in Figure 1, a conical shell composed of functionally graded material in supersonic airflow is considered. The semi-vertex angle, length, thickness, and radius at both ends of the conical shell are, respectively, represented by α, L, h, r and R. An orthogonal curvilinear coordinate system $(x,\ \theta,\ z)$ is located at the mid-surface of the conical shell, and the displacements in meridional (x), circumferential (θ), and radial (z) directions are represented by u, v and w, respectively. The airflow direction is along the x-axis.

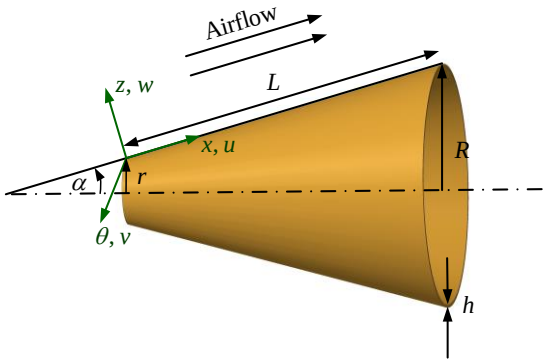

Figure 1. Schematic diagram of conical shell in supersonic flow.

The functionally graded conical shell is made from two materials; the inner layer of the conical shell is a ceramic material, and the outer layer of the conical shell is a metal material. The volume fractions of ceramic and metal are represented by V_c and V_m, respectively, and they can be written as follows:

$$V_m = \left(\frac{2z+h}{2h}\right)^p, V_c = 1 - V_m = 1 - \left(\frac{2z+h}{h}\right)^p, \tag{1}$$

where p is the index of the volume fraction, which is a positive number. Functionally graded material properties are temperature-dependent functions that can be given by

$$P(T) = P_0(P_{-1}T^{-1} + 1 + P_1T + P_2T^2 + P_3T^3), \tag{2}$$

where T is the temperature in the environment, and $P(T)$ is the material performance, including Young's modulus E, Poisson's ratio μ, density ρ, thermal expansion coefficient β and heat conduction coefficient k. P_0, P_{-1}, P_1, P_2 and P_3 are temperature-dependent coefficients of the material properties. The effective properties of composite materials in a specific temperature can be given by

$$P(z,T) = P_cV_c + P_mV_m, \tag{3}$$

Then,

$$\begin{aligned} &E(z,T) = E_c + (E_m - E_m)\left(\tfrac{2z+h}{h}\right)^p, \ \mu(z,T) = \mu_c + (\mu_m - \mu_m)\left(\tfrac{2z+h}{h}\right)^p, \\ &\rho(z,T) = \rho_c + (\rho_m - \rho_m)\left(\tfrac{2z+h}{h}\right)^p, \ \beta(z,T) = \beta_c + (\beta_m - \beta_m)\left(\tfrac{2z+h}{h}\right)^p, \\ &k(z,T) = k_c + (k_m - k_m)\left(\tfrac{2z+h}{h}\right)^p. \end{aligned} \tag{4}$$

2.2. Constrained Mode

According to Love's first approximation theory, the strain field on an arbitrary point of a conical shell is described as follows:

$$\begin{Bmatrix} \varepsilon_x \\ \varepsilon_\theta \\ \varepsilon_{x\theta} \end{Bmatrix} = \begin{Bmatrix} \varepsilon_{x,0} \\ \varepsilon_{\theta,0} \\ \varepsilon_{x\theta,0} \end{Bmatrix} + z\begin{Bmatrix} k_{x,0} \\ k_{\theta,0} \\ k_{x\theta,0} \end{Bmatrix}, \tag{5}$$

where $\{\varepsilon_{x,0} \quad \varepsilon_{\theta,0} \quad \varepsilon_{x\theta,0}\}^{\mathrm{T}}$ and $\{k_{x,0} \quad k_{\theta,0} \quad k_{x\theta,0}\}^{\mathrm{T}}$ are the mid-surface strains and surface curvature changes of the conical, respectively. They are stated as below:

$$\begin{aligned}
\varepsilon_{x,0} &= \frac{\partial u}{\partial x} \\
\varepsilon_{\theta,0} &= \frac{1}{r(x)}\frac{\partial v}{\partial \theta} + \frac{\sin\alpha}{r(x)}u + \frac{\cos\alpha}{r(x)}w \\
\varepsilon_{x\theta,0} &= \frac{\partial v}{\partial x} + \frac{1}{r(x)}\frac{\partial u}{\partial \theta} - \frac{\sin\alpha}{r(x)}v \\
k_{x,0} &= -\frac{\partial^2 w}{\partial x^2} \\
k_{\theta,0} &= -\frac{\sin\alpha}{r(x)}\frac{\partial w}{\partial x} - \frac{1}{r^2(x)}\frac{\partial^2 w}{\partial \theta^2} + \frac{\cos\alpha}{r^2(x)}\frac{\partial v}{\partial \theta} \\
k_{x\theta,0} &= 2\left(\frac{\sin\alpha}{r^2(x)}\frac{\partial w}{\partial \theta} - \frac{1}{r(x)}\frac{\partial^2 w}{\partial x \partial \theta} + \frac{\cos\alpha}{r(x)}\frac{\partial v}{\partial x} - \frac{\sin 2\alpha}{2r^2(x)}v\right),
\end{aligned} \tag{6}$$

where $r(x) = r + x\sin\alpha$.

Based on Hook's law, the components of stress in terms of strains of a functionally graded conical shell when thermal strain is considered can be expressed as

$$\begin{Bmatrix} \sigma_x \\ \sigma_\theta \\ \sigma_{x\theta} \end{Bmatrix} = \begin{bmatrix} Q_{11} & Q_{12} & 0 \\ Q_{21} & Q_{22} & 0 \\ 0 & 0 & Q_{66} \end{bmatrix} \left\{ \begin{Bmatrix} \varepsilon_x \\ \varepsilon_\theta \\ \varepsilon_{x\theta} \end{Bmatrix} - \begin{Bmatrix} \beta_x \\ \beta_\theta \\ \beta_{x\theta} \end{Bmatrix} \Delta T(z) \right\}, \tag{7}$$

where $\Delta T(z) = T - T_0$, $\beta_x = \beta_\theta = \beta(z,T)$, $\beta_{x\theta} = 0$, $T_0 = 300$ K.$\beta(z,T)$ is the thermal expansion coefficient. The stiffness coefficients Q_{ij} ($i, j = 1, 2, 6$) are expressed as

$$Q_{11} = Q_{22} = \frac{E(z,T)}{1-\mu^2(z,T)},\ Q_{12} = Q_{21} = \frac{\mu(z,T)E(z,T)}{1-\mu^2(z,T)},\ Q_{66} = \frac{E(z,T)}{2(1+\mu(z,T))}. \tag{8}$$

The kinetic energy of the functionally graded conical shell is expressed as

$$T_s = \frac{1}{2}\int_{-h/2}^{h/2}\int_0^{2\pi}\int_0^L \rho(\dot{u}^2 + \dot{v}^2 + \dot{w}^2)\cdot r(x)\mathrm{d}x\mathrm{d}\theta\mathrm{d}z. \tag{9}$$

The strain energy of the stretching and bending of the functionally graded conical shell can be given by

$$U_\varepsilon = \frac{1}{2}\int_0^L\int_0^{2\pi}\int_{-\frac{h}{2}}^{\frac{h}{2}} (\sigma_x\varepsilon_x + \sigma_\theta\varepsilon_\theta + \sigma_{x\theta}\varepsilon_{x\theta})r(x)\mathrm{d}x\mathrm{d}\theta\mathrm{d}z. \tag{10}$$

The potential energy due to the thermal stresses is described as [22]

$$U_{\Delta T} = \frac{1}{2}\int_0^L\int_0^{2\pi} N_x^T\left(\frac{\partial w}{\partial x}\right)^2 r(x)\mathrm{d}\theta\mathrm{d}\eta, \tag{11}$$

where N_x^T is expressed as

$$N_x^T = \int_{-\frac{h}{2}}^{\frac{h}{2}} [Q_{11}(z,T) + Q_{12}(z,T)]\beta(z,T)\Delta T(z)\mathrm{d}z. \tag{12}$$

Considering that the temperature only changes along the thickness direction, the equation of heat conduction can be stated as below:

$$-\frac{\mathrm{d}}{\mathrm{d}z}\left[k(z,T)\frac{\mathrm{d}T}{\mathrm{d}z}\right] = 0, \tag{13}$$

The thermal boundaries of the conical shell can be given by

$$T = T_m,\ z = h/2\ ;\ T = T_c,\ z = -h/2\ . \tag{14}$$

The solution of the equation, by means of polynomial series, can be written as [35]

$$T(z) = T_c + \Delta T \cdot \eta(z), \ \ \Delta T = T_m - T_c. \tag{15}$$

where

$$\begin{gathered}\eta(z) = \frac{1}{C}\left[\left(\frac{2z+h}{2h}\right) - \frac{k_{mc}}{(p+1)k_c}\left(\frac{2z+h}{2h}\right)^{p+1} + \frac{k_{mc}^2}{(2p+1)k_c^2}\left(\frac{2z+h}{2h}\right)^{2p+1}\right. \\ \left. - \frac{k_{mc}^3}{(3p+1)k_c^3}\left(\frac{2z+h}{2h}\right)^{3p+1} + \frac{k_{mc}^4}{(4p+1)k_c^4}\left(\frac{2z+h}{2h}\right)^{4p+1} - \frac{k_{mc}^5}{(5p+1)k_c^5}\left(\frac{2z+h}{2h}\right)^{5p+1}\right], \\ C = 1 - \frac{k_{mc}}{(p+1)k_c} + \frac{k_{mc}^2}{(2p+1)k_c^2} - \frac{k_{mc}^3}{(3p+1)k_c^3} + \frac{k_{mc}^4}{(4p+1)k_c^4} - \frac{k_{mc}^5}{(5p+1)k_c^5},\end{gathered} \tag{16}$$

where $k_{mc} = k_m - k_c$. For thin conical shells, the temperature distribution can be considered linear:

$$\eta(z) = \left(\frac{2z+h}{2h}\right). \tag{17}$$

The constrained modes of the composite conical shell are obtained using the Rayleigh–Ritz method. The displacement function of the structure is expressed as

$$\begin{cases} u(x,\theta,t) = U_n(x)\cos(n\theta)\sin\omega t = \sum\limits_{J=1}^{N} a_{Jn}\varphi_{u,J}(x)\cos(n\theta)\sin\omega t \\ v(x,\theta,t) = V_n(x)\sin(n\theta)\sin\omega t = \sum\limits_{J=1}^{N} b_{Jn}\varphi_{v,J}(x)\sin(n\theta)\sin\omega t \\ w(x,\theta,t) = W_n(x)\cos(n\theta)\sin\omega t = \sum\limits_{J=1}^{N} c_{Jn}\varphi_{w,J}(x)\cos(n\theta)\sin\omega t \end{cases}, \tag{18}$$

where n is circumferential wave number, and ω is natural frequency. $U_n(x)$, $V_n(x)$ and $W_n(x)$ are the meridional modal functions used to described the vibrational mode in the longitudinal direction, which can be approximated using the characteristic orthogonal polynomials satisfying the boundary conditions. N is the number of truncated terms used in practical calculation,a_{Jn}, b_{Jn} and c_{Jn} are the unknown coefficients, and $\varphi_{J,u}(x)$, $\varphi_{J,v}(x)$ and $\varphi_{J,w}(x)$ are the characteristic orthogonal polynomials which can be generated using the Gram–Schmidt procedure according to the boundary conditions. More details about the characteristic orthogonal polynomials are provided in the literature [36].

The Rayleigh quotient is given by

$$\omega^2 = \frac{(U_\varepsilon + U_{\Delta T})_{\max}}{(T_s)_{\max}}, \tag{19}$$

and

$$\frac{\partial\omega^2}{\partial a_{Jn}} = 0, \frac{\partial\omega^2}{\partial b_{Jn}} = 0, \frac{\partial\omega^2}{\partial c_{Jn}} = 0, J = 1, 2, 3\cdots N. \tag{20}$$

Substituting expression (9)–(11) and (18) into the above equation, the eigenvalue equation of the conical shell is obtained:

$$\left[\omega^2\mathbf{M}_R - \mathbf{K}_{R\varepsilon} - \mathbf{K}_{R\Delta T}\right]\begin{Bmatrix}\mathbf{a}\\ \mathbf{b}\\ \mathbf{c}\end{Bmatrix} = 0. \tag{21}$$

Then, the frequency equation of conical shell is described by

$$\left|\omega^2\mathbf{M}_R - \mathbf{K}_{R\varepsilon} - \mathbf{K}_{R\Delta T}\right| = 0 \tag{22}$$

where $\mathbf{M}_R$ is $3N \times 3N$ mass matrix of the conical shell, $\mathbf{K}_{R\varepsilon}$ is $3N \times 3N$ stiffness matrix of the conical shell, and $\mathbf{K}_{R\Delta T}$ is $3N \times 3N$ thermal stiffness matrix of the conical shell. The

unknown vector of coefficients **a**, **b** and **c** in the mode function of the conical shell under classical conditions can be calculated from Equation (21). Then, the displacement function of the functionally graded conical shell at a specific temperature can be determined.

2.3. Dynamic Equation

Based on the mode function of the functionally graded conical shell obtained using the Rayleigh–Ritz method, the displacement components of the conical shell are stated as below:

$$\begin{cases} u(x,\theta,t) = \sum\limits_{i=1}^{m}\sum\limits_{j=1}^{n} U_{ij}(x,\theta)q_{ij}^{u}(t) = \mathbf{U}\mathbf{q}_u(t) \\ v(x,\theta,t) = \sum\limits_{i=1}^{m}\sum\limits_{j=1}^{n} V_{ij}(x,\theta)q_{ij}^{v}(t) = \mathbf{V}\mathbf{q}_v(t) \\ w(x,\theta,t) = \sum\limits_{i=1}^{m}\sum\limits_{j=1}^{n} W_{ij}(x,\theta)q_{ij}^{w}(t) = \mathbf{W}\mathbf{q}_w(t) \end{cases}, \tag{23}$$

where m is the modal truncation number. **U**, **V** and **W** are the mode functions in meridional, circumferential and radial directions, respectively. $\mathbf{q}_u$, $\mathbf{q}_v$ and $\mathbf{q}_w$ are the generalized coordinates.

According to the linear piston theory with a curvature correction term, the aerodynamic pressure generated by supersonic flowing through the outer surface of the functionally graded conical shell is given by [2,32]:

$$\Delta p = \frac{\gamma p_\infty M_\infty^2}{\left(M_\infty^2-1\right)^{1/2}}\left[\frac{M_\infty^2-2}{M_\infty^2-1}\frac{1}{\alpha_\infty M_\infty}\frac{\partial w}{\partial t} + \frac{\partial w}{\partial x} - \frac{w}{2r(x)\left(M_\infty^2-1\right)^{1/2}}\right], \tag{24}$$

where, p_∞, γ, M_∞ and α_∞ are the free-stream static pressure, air-specific heat ratio, Mach number and speed of sound, respectively. It should be noted that the linearized first-order potential theory is valid for $\sqrt{2} < M_\infty < 5$. Moreover, since the flow over a shell behind the attached shock wave is nonuniform, the constant Mach number is effective for a sufficiently short shell [19].

The virtual work caused by the aerodynamic load is written as

$$\delta W = -\int_0^L \int_0^{2\pi} (\Delta p \delta w)\cdot r(x)\mathrm{d}x\mathrm{d}\theta = Q_p \delta q_w, \tag{25}$$

where the expression of generalized force Q_p is

$$\begin{aligned} Q_p \quad &= \frac{\gamma p_\infty M_\infty^2}{\left(M_\infty^2-1\right)^{1/2}}\int_0^L\int_0^{2\pi}\left[\mathbf{W}\frac{\partial \mathbf{W}^T}{\partial x}r(x) - \frac{1}{2\left(M_\infty^2-1\right)^{1/2}}\mathbf{W}\mathbf{W}^T\right]\mathrm{d}x\mathrm{d}\theta\mathbf{q}_w \\ &+\int_0^L\int_0^{2\pi}\left[\frac{M_\infty^2-2}{M_\infty^2-1}\frac{r(x)}{\alpha_\infty M_\infty}\mathbf{W}\mathbf{W}^T\right]\mathrm{d}x\mathrm{d}\theta\dot{\mathbf{q}}_w. \end{aligned} \tag{26}$$

Substituting expressions (9)–(11), (23) and (26) into Lagrange equations,

$$\frac{\mathrm{d}}{\mathrm{d}t}\left(\frac{\partial L}{\partial \dot{q}_p}\right) - \frac{\partial L}{\partial q_p} = Q_p, \tag{27}$$

where $L = T - U_\varepsilon - U_{\Delta T}$, $p = u,\ v,\ w$. The dynamic equation of the functionally graded conical shell can be described by the following equation:

$$\mathbf{M}\ddot{\mathbf{X}} + \mathbf{C}_{\Delta P}\dot{\mathbf{X}} + (\mathbf{K}_\varepsilon + \mathbf{K}_{\Delta T} + \mathbf{K}_{\Delta p})\mathbf{X} = 0, \tag{28}$$

where $\mathbf{X} = \left[\mathbf{q}_u^T,\ \mathbf{q}_v^T,\ \mathbf{q}_w^T\right]^T$. $\mathbf{K}_\varepsilon$ and $\mathbf{M}$ are, respectively, the stiffness matrix and mass matrix of the functionally graded conical shell. $\mathbf{K}_{\Delta P}$ and $\mathbf{C}_{\Delta P}$ are, respectively, the stiffness matrix and damping matrix related to aerodynamic load, and $\mathbf{K}_{\Delta T}$ is the stiffness matrix related to thermal load.

The frequency equation of the system can be described by

$$\left|\mathbf{M}\Omega^2 + \mathbf{C}_{\Delta P}\Omega + (\mathbf{K}_{\varepsilon} + \mathbf{K}_{\Delta T} + \mathbf{K}_{\Delta p})\right| = 0. \tag{29}$$

The complex eigenvalue Ω_{mn} of the structure can be obtained from the above equation (29), and the corresponding frequency ω_{mn} of the conical shell can be expressed by the imaginary part of the eigenvalue:

$$\omega_{mn} = \sqrt{[\mathrm{Im}(\Omega_{mn})]^2}. \tag{30}$$

As the free-stream static pressure p_∞ increases gradually, the two adjacent natural frequencies of the structure converge, which can cause flutter [10]. Additionally, the corresponding free-stream static pressure is known as critical free-stream static pressure.

3. Comparison and Convergence Studies

To verify the effectiveness of the present solution procedure, comparison and convergence studies have been carried out. First, the natural frequencies of a functionally graded conical shell under clamped–clamped boundaries at both ends are obtained and compared with the previous literature. The comparison results are shown in Table 1. It can be observed from Table 1 that with the increase in the terms of the orthogonal polynomials truncated, the dimensionless frequency parameters converge, and when $N = 10$, the present result and those from the literature [23] are in good agreement.

Table 1. Dimensionless frequency parameters ($\overline{\omega} = \omega R\sqrt{\rho(1-\mu^2)/E}$) of a functionally graded conical shell under clamped–clamped boundary conditions ($m = 1$, $n = 1$, $h/r = 0.01$, $p = 1$).

	α	Shakouri [23]	Present Results					
			$N = 5$	$N = 6$	$N = 7$	$N = 8$	$N = 9$	$N = 10$
$L/r = 1$	30°	0.85746	0.87708	0.86008	0.85790	0.85765	0.85740	0.85740
	60°	0.44767	0.45785	0.44823	0.44817	0.44769	0.44766	0.44766
$L/r = 5$	30°	0.30770	0.31969	0.31730	0.30935	0.30914	0.30796	0.30794
	60°	0.14467	0.16803	0.15799	0.14986	0.14682	0.14511	0.14493

Second, the correctness of the flutter stabilities derived in the present investigations are verified. The critical dynamic pressure parameter $\lambda(\lambda = 12(1-\mu^2)\gamma p_\infty M_\infty^2 r^3/Eh^3\sqrt{M_\infty^2-1})$ of the simply supported conical shell investigated in the literature [32] is counted, and its convergence is analyzed. It can be found from Figure 2 that the natural frequencies and dynamic pressure parameter have gradually converged with the increase in the modal truncation numbers m. In addition, it can be seen that the critical dynamic pressure parameter calculated here is $\lambda_{cr} = 556$, which is in agreement with the previous result of $\lambda_{cr} = 566.4$ [32].

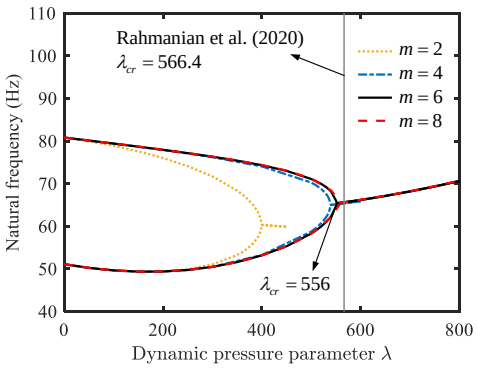

Figure 2. Mode convergence and comparison study for the aerothermoelastic analysis with result reported in the literature [32].

4. Numerical Results and Discussions

The aerothermoelastic characteristics of a conical shell with free–clamped boundaries are investigated in the section. The inner and outer layers' materials are Si3N4 and SUS304, respectively, and the material coefficients of the functionally graded conical shell studied in the paper are shown in Table 2. The free-stream parameters are $\gamma = 1.4$, $a_\infty = 213.6$ m/s, $M_\infty = 3$. The physical parameters for the conical shell are as below: $\alpha = 30°$, $L/r = 1$, $h/r = 0.01$.

Table 2. Material properties of a functionally graded conical shell.

Property		P_{-1}	P_0	P_1	P_2	P_3
E (pa)	SUS304	0	201.04×10^9	3.079×10^{-4}	-6.534×10^{-7}	0
	Si_3N_4	0	348.43×10^9	-3.070×10^{-4}	2.130×10^{-7}	-8.946×10^{-11}
μ	SUS304	0	0.31	0	0	0
	Si_3N_4	0	0.24	0	0	0
ρ (kg/m^3)	SUS304	0	8166	0	0	0
	Si_3N_4	0	2370	0	0	0
β (1/K)	SUS304	0	12.330×10^{-6}	8.086×10^{-4}	0	0
	Si_3N_4	0	5.8723×10^{-6}	9.095×10^{-4}	0	0
k (W/m°K)	SUS304	0	15.379	0	0	0
	Si_3N_4	0	13.723	0	0	0

4.1. Natural Vibration Characteristics Analysis

In this section, the effects of temperature change and free-stream static pressure on the fundamental frequency of the composite conical shell are analyzed. As shown in Figure 3, the influence of temperature change on the natural frequency of a conical shell under different volume fraction indices is studied. It can be observed from the figure that in a thermal environment, the natural frequency solved based on the linear temperature hypothesis is basically consistent with the natural frequency calculated based on the polynomial series representation of the temperature distribution. It can be concluded that the linear temperature distribution is reasonable for thin-walled conical shells. Additionally, as the temperature difference between the upper and lower surfaces increases, the natural frequency of the conical shell first decreases slowly, then rapidly, and finally becomes zero. The temperature change corresponding to the zero natural frequency is the critical buckling temperature change of the structure, represented by ΔT_{cr}. In addition, it can be also found that the fundamental frequency of the conical shell increases as the volume fraction increases, and the critical buckling temperature change is proportional to the index of volume fraction.

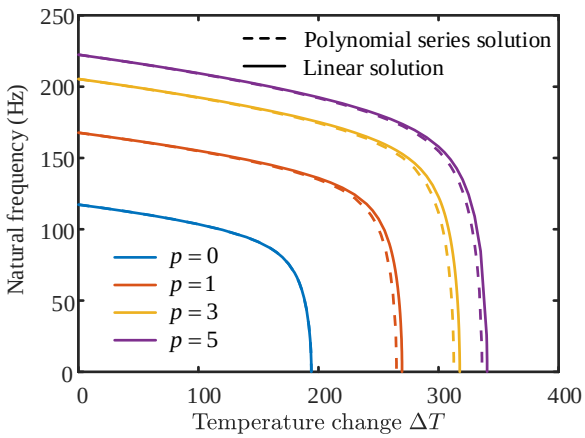

Figure 3. The influence of temperature change on the natural frequency of a conical shell under different volume fraction indices.

The influence of free-stream static pressure on the natural frequency of the conical shell is studied in Figure 4. As is shown in the figure, for the conical shell under free–clamped boundary conditions, with the increase in p_∞, the natural frequencies of the first mode decrease gradually and finally become zero, the natural frequencies of second mode decrease gradually but remain basically stable, the natural frequencies of third order increase gradually, and the natural frequencies of fourth order decrease gradually. When the free-stream static pressure p_∞ is further increased, the natural frequencies of the third and fourth modes merge into a single mode. When two adjacent natural frequencies converge with the increase in p_∞, the conical shell loses stability and flutters.

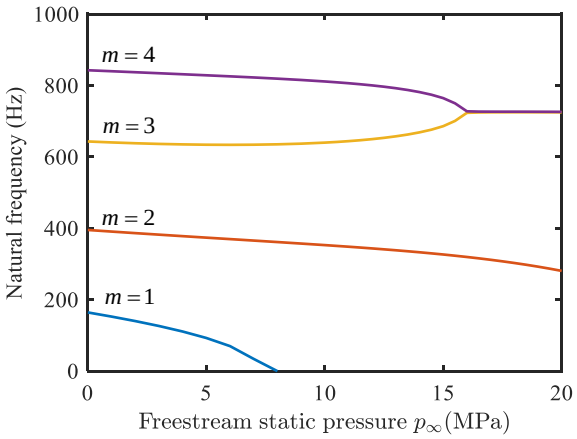

Figure 4. Natural frequency versus free-stream static pressure for a conical shell with different modes (p = 1).

4.2. Aerothermoelastic Stability Analysis

The influence of the structural parameters of a conical shell, such as the ratio of length to radius, ratio of thickness to radius, the semi-vertex angle, as well as thermal and aerodynamic loads, on its aerothermoelastic stability is carried out.

Figure 5 depicts the influence of the ratio of length to radius of the conical shell on the thermal buckling stability at different volume fraction indices. As is shown in Figure 5, the critical buckling temperature change ΔT_{cr} of the structure slightly increases with the increase in the ratio of length to radius.

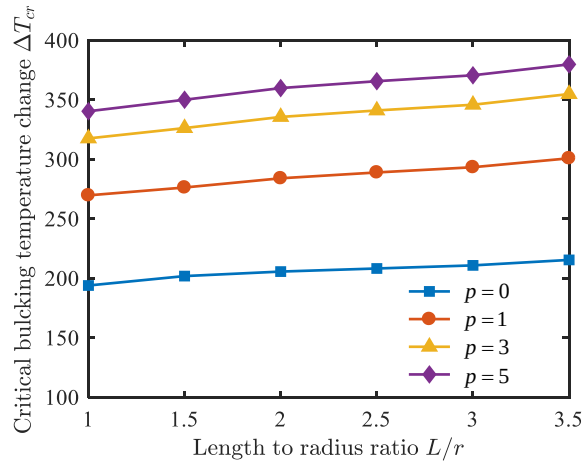

Figure 5. Influence of the length-to-radius ratio of the conical shell on critical buckling temperature change.

Variations in the critical buckling temperature change with the ratio of thickness to radius under different volume fraction indices are shown in Figure 6. It can be found

that with the increase in the thickness-to-radius ratio of conical shell, the critical buckling temperature change of the structure will gradually increase, and the structure is less prone to thermal buckling. As can be observed from the comparison between Figures 5 and 6, the ratio of thickness to radius has a more significant influence on thermal buckling stability than the ratio of length to radius. In addition, it can be found from Figures 5 and 6 that the ΔT_{cr} of the conical shell is proportional to the volume fraction of the functionally graded material.

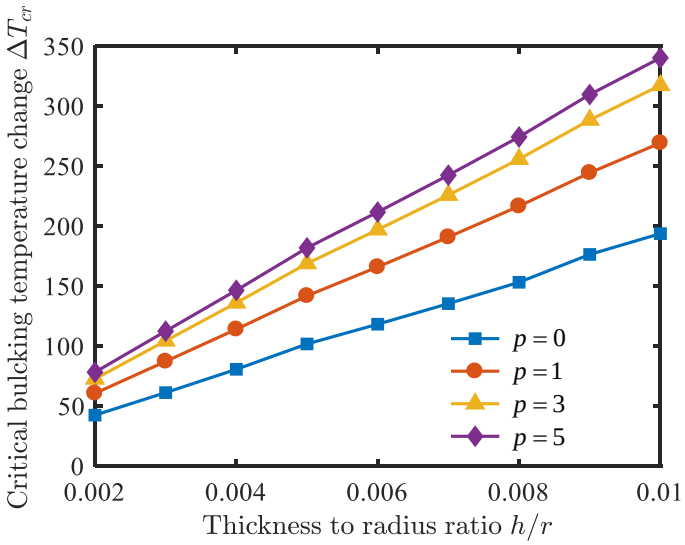

Figure 6. Influence of the thickness-to-radius ratio of the conical shell on critical buckling temperature change.

As shown in Figure 7, the variation of ΔT_{cr} is analyzed when the semi-vertex angle α increases from 10° to 60°. It can be clearly observed that when the semi-vertex angle of the structure is small ($\alpha \leq 15°$), the critical buckling temperature change is little affected by the semi-vertex angle; when the semi-vertex angle is large ($\alpha \geq 15°$), the critical buckling temperature change will gradually decrease with the increase in the semi-vertex angle. It can be shown that the smaller the semi-vertex angle of the structure, the better the thermal buckling stability of the conical shell.

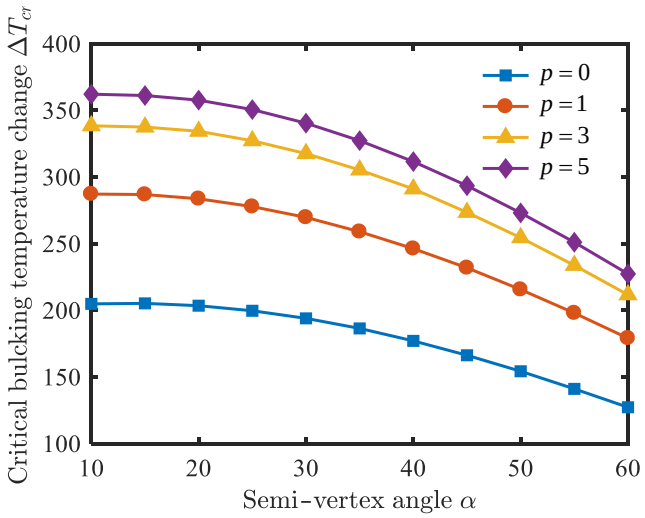

Figure 7. Influence of the semi-vertex angle of the conical shell on critical buckling temperature change.

According to the analysis in Figure 4, for a conical shell under free–clamped boundaries, the free-stream static pressure when the natural frequencies of third and fourth order converge is the critical free-stream static pressure. Based on the above conclusions, the effects of various factors on the flutter stability of conical shell are studied in Figures 8–12.

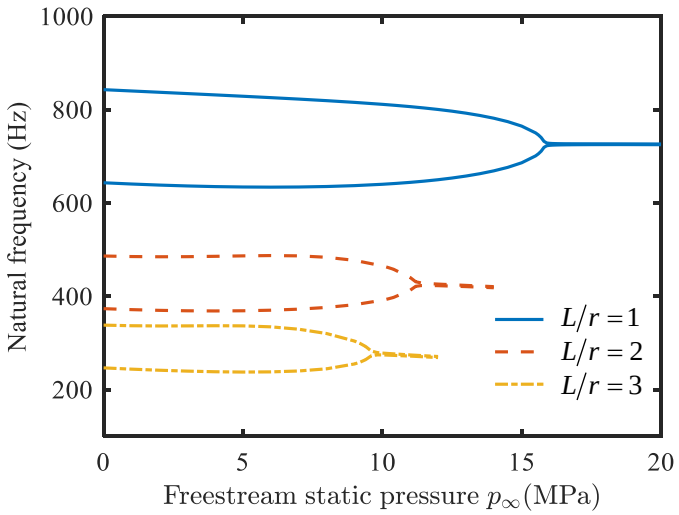

Figure 8. Influence of the length-to-radius ratio of the conical shell on critical free-stream static pressure ($p = 1$).

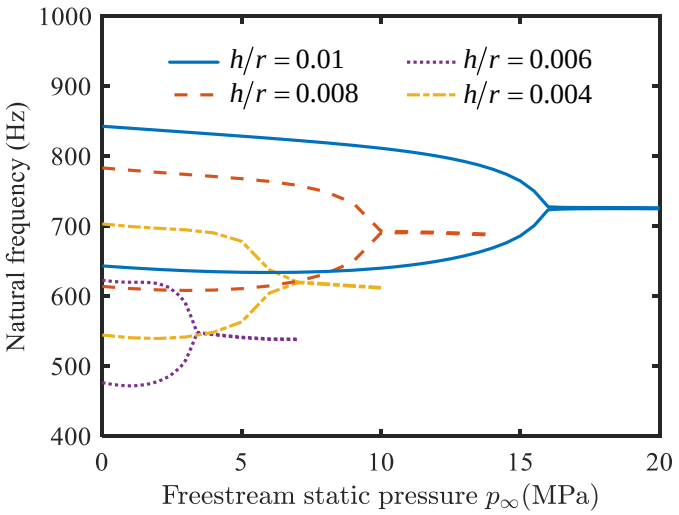

Figure 9. Influence of the thickness-to-radius ratio of the conical shell on critical free-stream static pressure ($p = 1$).

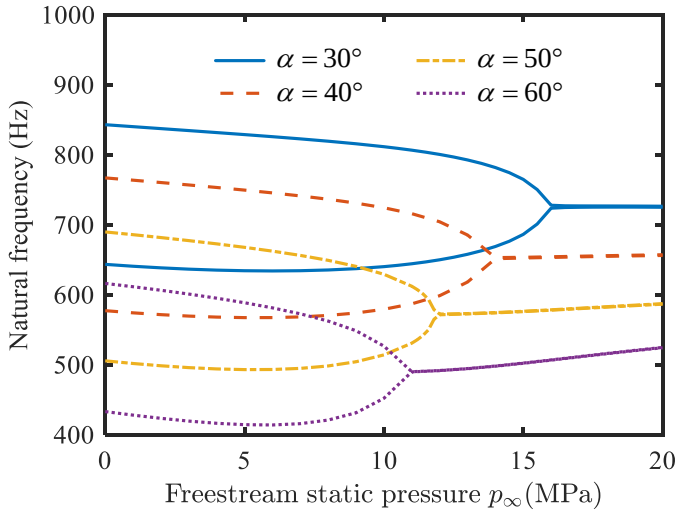

Figure 10. Influence of semi-vertex angle of conical shell on critical free-stream static pressure (p = 1).

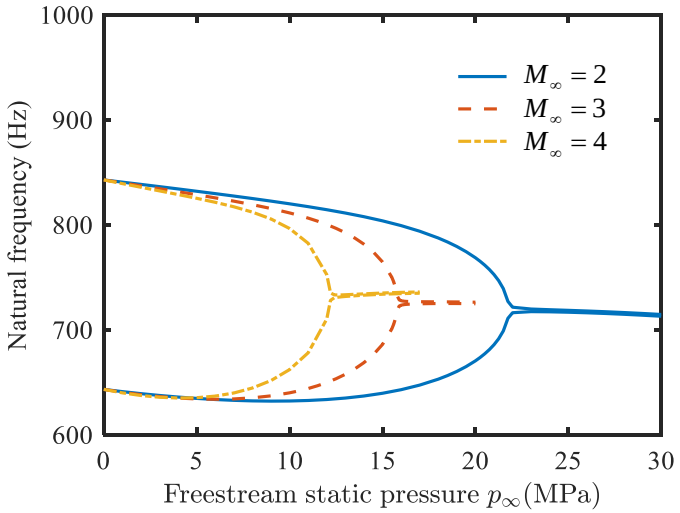

Figure 11. Influence of Mach number on critical free-stream static pressure (p = 1).

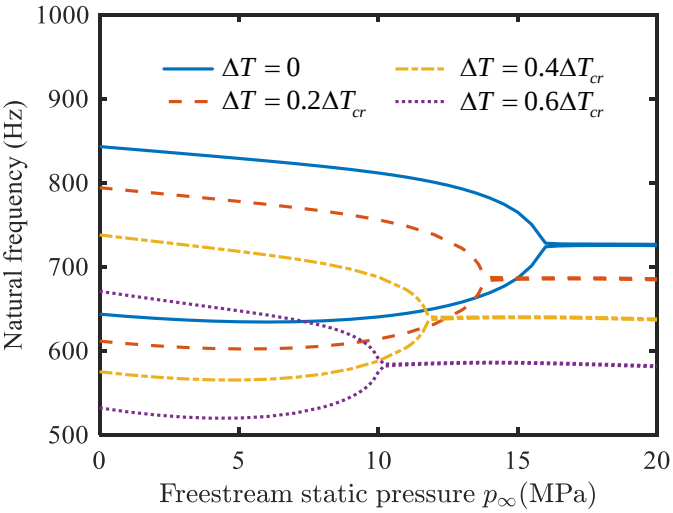

Figure 12. Influence of temperature change on critical free-stream static pressure (p = 1).

Figure 8 analyzes the effect of the length-to-radius ratio of the conical shell on the critical free-stream static pressure. From the figure, it can be found that the increase in the length-to-radius ratio leads to a decrease in the critical flutter pressure. In addition, with the increase in the length-to-radius ratio, the natural frequencies of the conical shell decrease. Figure 9 describes the effect of the thickness-to-radius ratio of the conical shell on the critical free-stream static pressure. It can be found from the figure that the critical free-stream static pressure and the natural frequencies increase as the ratio of radius to thickness increases. The influence of the semi-vertex angle of the conical shell on the critical free-stream static pressure is given in Figure 10. It can be observed that with the increase in the semi-vertex angle, the critical free-stream static pressure decreases accordingly. Furthermore, the natural frequency is inversely proportional to the semi-vertex angle.

Figure 11 describes the variation of the critical free-stream static pressure of conical shell with Mach number. It can be observed from Figure 11 that as the Mach number increases, the critical free-stream static pressure decreases. The variations in the critical free-stream static pressure of the conical shell with different temperature change ΔT are studied. As shown in Figure 12, the flutter stability of the composite conical shell under the four temperature conditions of $\Delta T = 0$, $\Delta T = 0.2\Delta T_{cr}$, $\Delta T = 0.4\Delta T_{cr}$ and $\Delta T = 0.6\Delta T_{cr}$ is analyzed, respectively. It is found that as the temperature change increases, the critical free-stream static pressure gradually decreases.

5. Conclusions

In the paper, a study of the aerothermoelastic characteristics of a conical shell in supersonic airflow has been carried out. According to the Love's first approximation shell theory, a linear piston theory with a curvature correction term and linear temperature assumption, the dynamics model of the conical shell is established by a Lagrange equation. It is worth noting that the constrained modes of the structure are obtained using the Rayleigh–Ritz method by taking the characteristic orthogonal polynomial series as the admissible functions. According to the influence of temperature change and free-stream static pressure on the natural frequency of the functionally graded conical shell, the influence of temperature change and free-stream static pressure on the fundamental frequencies of the functionally graded conical shell is studied. The conclusions can be summarized as follows:

(1) For thin-walled conical shells, the linear temperature assumption is reasonable.
(2) With an increase in temperature change, the fundamental frequency of the conical shell decreases gradually, and finally drops to zero. As the static pressure of the free-stream increases, two adjacent natural frequencies converge, which can cause flutter.
(3) The natural frequencies of the conical shell are proportional to the ratio of thickness to radius, and inversely proportional to the ratio of length to radius and semi-vertex angle.
(4) With an increase in the length-to-radius ratio, the critical buckling temperature change increases slightly, and the critical free-stream static pressure decreases obviously; the critical buckling temperature change and the critical free-stream static pressure are enhanced by raising the thickness-to-radius ratio; the critical buckling temperature change and the critical free-stream static pressure decrease when the semi-vertex angle is enhanced.
(5) The critical flutter pressure of conical shell is intensified with a decrease in the Mach number and temperature.

Author Contributions: Conceptualization, M.W., C.Z. and S.S.; methodology, C.Z. and Y.Y.; software, M.W., L.Z. and Y.Y.; validation, C.Z. and Y.Y.; writing—original draft preparation, M.W. and L.Z.; writing—review and editing, C.Z. and S.S.; supervision, S.S. All authors have read and agreed to the published version of the manuscript.

Funding: This research was funded by National Natural Science Foundation of China (Grant Nos. 11802129 and 12172307), Shandong Provincial Natural Science Foundation of China (Grant No. ZR2020QA039), and the Opening Project of Applied Mechanics and Structure Safety Key Laboratory of Sichuan Province (Grant No. SZDKF-202103).

Institutional Review Board Statement: Not applicable.

Informed Consent Statement: Not applicable.

Data Availability Statement: Not applicable.

Acknowledgments: The authors would like to thank colleagues of AVIC Research Institute for Special Structures of Aeronautical Composites for helpful discussions on topics related to this work.

Conflicts of Interest: The authors declare no conflict of interest.

References

1. Amabili, M.; Pellicano, F. Nonlinear supersonic flutter of circular cylindrical shells. *AIAA J.* **2001**, *39*, 564–573. [CrossRef]
2. Amabili, M.; Pellicano, F. Multimode approach to nonlinear supersonic flutter of imperfect circular cylindrical shells. *J. Appl. Mech.-Trans. ASME* **2002**, *69*, 117–129. [CrossRef]
3. Haddadpour, H.; Mahmoudkhani, S.; Navazi, H.M. Supersonic flutter prediction of functionally graded cylindrical shells. *Compos. Struct.* **2008**, *83*, 391–398. [CrossRef]
4. Shin, W.H.; Oh, I.K.; Lee, I. Nonlinear flutter of aerothermally buckled composite shells with damping treatments. *J. Sound Vib.* **2009**, *324*, 556–569. [CrossRef]
5. Song, Z.G.; Li, F.M. Aerothermoelastic analysis and active flutter control of supersonic composite laminated cylindrical shells. *Compos. Struct.* **2013**, *106*, 653–660. [CrossRef]
6. Sabri, F.; Lakis, A.A. Efficient hybrid finite element method for flutter prediction of functionally graded cylindrical shells. *J. Vib. Acoust.-Trans. ASME* **2014**, *136*, 011002. [CrossRef]
7. Bochkarev, S.A.; Lekomtsev, S.V.; Matveenko, V.P. Aeroelastic stability of heated functionally graded cylindrical shells containing fluid. *Mech. Adv. Mater. Struct.* **2017**, *24*, 1391–1400. [CrossRef]
8. Asadi, H. Numerical simulation of the fluid-solid interaction for CNT reinforced functionally graded cylindrical shells in thermal environments. *Acta Astronaut.* **2017**, *138*, 214–224. [CrossRef]
9. Zhang, L.W.; Song, Z.G.; Liew, K.M. Modeling aerothermoelastic properties and active flutter control of nanocomposite cylindrical shells in supersonic airflow under thermal environments. *Comput. Methods Appl. Mech. Eng.* **2017**, *325*, 416–433. [CrossRef]
10. Chai, Y.Y.; Song, Z.G.; Li, F.M. Investigations on the aerothermoelastic properties of composite laminated cylindrical shells with elastic boundaries in supersonic airflow based on the Rayleigh-Ritz method. *Aerosp. Sci. Technol.* **2018**, *82–83*, 534–544. [CrossRef]
11. Lin, H.G.; Cao, D.Q.; Shao, C.H. An admissible function for vibration and flutter studies of FG cylindrical shells with arbitrary edge conditions using characteristic orthogonal polynomials. *Compos. Struct.* **2018**, *185*, 748–763. [CrossRef]
12. Bochkarev, S.A.; Lekomtsev, S.V. Stability of functionally graded circular cylindrical shells under combined loading. *Mech. Compos. Mater.* **2019**, *55*, 349–362. [CrossRef]
13. Fazilati, J.; Khalafi, V.; Shahverdi, H. Three-dimensional aero-thermo-elasticity analysis of functionally graded cylindrical shell panels. *Proc. Inst. Mech. Eng. Part G J. Aerosp. Eng.* **2019**, *233*, 1715–1727. [CrossRef]
14. Mahmoudkhani, S. Aerothermoelastic analysis of imperfect FG cylindrical shells in supersonic flow. *Compos. Struct.* **2019**, *225*, 111160. [CrossRef]
15. Guo, H.L.; Zur, K.K.; Ouyang, X. New insights into the nonlinear stability of nanocomposite cylindrical panels under aero-thermal loads. *Compos. Struct.* **2023**, *303*, 116231. [CrossRef]
16. Mei, C.; Abdel-Motagly, K.; Chen, R. A review of nonlinear panel flutter at supersonic and hypersonic speeds. *Appl. Mech. Rev.* **1999**, *52*, 321–332. [CrossRef]
17. Shishaeva, A.; Aksenov, A.; Vedeneev, V. The effect of external perturbations on nonlinear panel flutter at low supersonic speed. *J. Fluids Struct.* **2022**, *111*, 103570. [CrossRef]
18. Abdukhakimov, F.A.; Vedeneev, V.V. Effect of Yaw Angle on Flutter of Rectangular Plates at Low Supersonic Speeds. *AIAA J.* **2022**, *60*, 4256–4266. [CrossRef]
19. Vedeneev, V.V.; Nesterov, V.A. Effect of Nonequilibrium Reacting Flow on Flutter at Hypersonic Flight Speed. *AIAA J.* **2019**, *57*, 2222–2226. [CrossRef]
20. Bhangale, R.K.; Ganesan, N.; Padmanabhan, C. Linear thermoelastic buckling and free vibration behavior of functionally graded truncated conical shells. *J. Sound Vib.* **2006**, *292*, 341–371. [CrossRef]
21. Naj, R.; Boroujerdy, M.S.; Eslami, M.R. Thermal and mechanical instability of functionally graded truncated conical shells. *Thin-Walled Struct.* **2008**, *46*, 65–78. [CrossRef]
22. Talebitooti, M. Thermal effect on free vibration of ring-stiffened rotating graded conical shell with clamped ends. *Mech. Adv. Mater. Struct.* **2016**, *25*, 155–165. [CrossRef]
23. Shakouri, M. Free vibration analysis of functionally graded rotating conical shells in thermal environment. *Compos. Part B-Eng.* **2019**, *163*, 574–584. [CrossRef]
24. Dixon, S.C.; Hudson, M.L. *Flutter, Vibration, and Buckling of Truncated Orthotropic Conical Shells with Generalized Elastic Edge Restraint*; TN D-5759; NASA: Washington, DC, USA, 1970.
25. Bismarcknasr, M.N.; Costasavio, H.R. Finite-element solution of the supersonic flutter of conical shells. *AIAA J.* **1979**, *17*, 1148–1150. [CrossRef]

26. Vasil'ev, A.V. Flutter of conical shells under external flow of a supersonic gas. *Mosc. Univ. Mech. Bull.* **2015**, *70*, 23–27. [CrossRef]
27. Sabri, F.; Lakis, A.A. Hybrid finite element method applied to supersonic flutter of an empty or partially liquid-filled truncated conical shell. *J. Sound Vib.* **2010**, *329*, 302–316. [CrossRef]
28. Zhang, R.; Yang, Z.; Gao, Y. The flutter of truncated conical shell subjected to internal supersonic air flow. *Multidiscip. Model. Mater. Struct.* **2014**, *10*, 18–35.
29. Mehri, M.; Asadi, H.; Wang, Q. On dynamic instability of a pressurized functionally graded carbon nanotube reinforced truncated conical shell subjected to yawed supersonic airflow. *Compos. Struct.* **2016**, *153*, 938–951. [CrossRef]
30. Bakhtiari, M.; Lakis, A.A.; Kerboua, Y. Nonlinear supersonic flutter of truncated conical shells. *J. Mech. Sci. Technol.* **2020**, *34*, 1375–1388. [CrossRef]
31. Afshari, H.; Ariaseresht, Y.; Koloor, S.S.R.; Amirabadi, H.; Bidgoli, M.O. Supersonic flutter behavior of a polymeric truncated conical shell reinforced with agglomerated CNTs. *Waves Random Complex Media* **2022**, 23. [CrossRef]
32. Rahmanian, M.; Javadi, M. A unified algorithm for fully-coupled aeroelastic stability analysis of conical shells in yawed supersonic flow to identify the effect of boundary conditions. *Thin-Walled Struct.* **2020**, *155*, 106910. [CrossRef]
33. Mahmoudkhani, S.; Haddadpour, H.; Navazi, H.M. Supersonic flutter prediction of functionally graded conical shells. *Compos. Struct.* **2010**, *92*, 377–386. [CrossRef]
34. Hao, Y.X.; Yang, S.W.; Zhang, W.; Yao, M.H.; Wang, A.W. Flutter of high-dimension nonlinear system for a FGM truncated conical shell. *Mech. Adv. Mater. Struct.* **2018**, *25*, 47–61. [CrossRef]
35. Shen, H.S.; Noda, N. Postbuckling of FGM cylindrical shells under combined axial and radial mechanical loads in thermal environments. *Int. J. Solids Struct.* **2005**, *42*, 4641–4662. [CrossRef]
36. Sun, S.; Cao, D.; Han, Q. Vibration studies of rotating cylindrical shells with arbitrary edges using characteristic orthogonal polynomials in the rayleigh–ritz method. *Int. J. Mech. Sci.* **2013**, *68*, 180–189. [CrossRef]